

## **Blind prediction of a cyclic pushover test on a two-storey masonry assemblage a comparative study**

Messali, Francesco; Pari, Manimaran; Esposito, Rita; Rots, Jan; den Hertog, D

**Publication date**

2018

**Document Version**

Accepted author manuscript

**Published in**

Proceedings of the 16th European Conference on Earthquake Engineering

**Citation (APA)**

Messali, F., Pari, M., Esposito, R., Rots, J., & den Hertog, D. (2018). Blind prediction of a cyclic pushover test on a two-storey masonry assemblage: a comparative study. In *Proceedings of the 16th European Conference on Earthquake Engineering: Thessaloniki, Greece*

**Important note**

To cite this publication, please use the final published version (if applicable).  
Please check the document version above.

**Copyright**

Other than for strictly personal use, it is not permitted to download, forward or distribute the text or part of it, without the consent of the author(s) and/or copyright holder(s), unless the work is under an open content license such as Creative Commons.

**Takedown policy**

Please contact us and provide details if you believe this document breaches copyrights.  
We will remove access to the work immediately and investigate your claim.

## **BLIND PREDICTIONS OF A CYCLIC PUSHOVER TEST ON A TWO-STOREY MASONRY ASSEMBLAGE: A COMPARATIVE STUDY**

Francesco MESSALI<sup>1</sup>, Manimaran PARI<sup>2</sup>, Rita ESPOSITO<sup>3</sup>, Jan ROTS<sup>4</sup>, Dick DEN HERTOG<sup>5</sup>

### **ABSTRACT**

In recent years induced seismicity in the north of the Netherlands has considerably increased. The built environment in the region mainly consists of unreinforced masonry (URM) buildings. Those buildings were not designed for seismic loads and have specific characteristics, that limit their seismic performance. In early 2017 a quasi-static cyclic pushover test on a calcium silicate element assemblage was carried out at Delft University of Technology. The assembled structure is representative of a typical terraced house built after the 1980's in the Netherlands. The test was selected for a blind prediction contest, with the aim of (i) sharing the knowledge between consultant companies, (ii) improving the understanding of the structural behaviour of a typical URM structure, and (iii) contributing to the development of the Dutch guidelines for the seismic assessment of existing buildings. Nine engineering consultants working for the seismic assessment of the Groningen building stock participated to the contest. The predictions were characterised by different modelling methodologies, from analytical computations to equivalent-frame based or full finite element analyses.

The paper presents an analysis of the submitted predictions, in an anonymous format, and trends related to the adopted analysis methodology are identified. On average, the predictions can provide a good estimate of the experimental outcomes, but a large scatter between the predicted results is observed. Finally, the received predictions have been used to assess the seismic vulnerability of the tested structure according to the recent Dutch seismic guidelines and with different assessment procedures: the assessments based on the numerical analyses were overall consistent to that based on the experimental outcomes.

*Keywords: Blind test prediction; Unreinforced masonry; Full-scale building; Seismic assessment; Pushover.*

### **1. INTRODUCTION**

In recent years, the northern part of the Netherlands has been facing seismic risk due to gas extraction. Several induced earthquakes of low magnitude occurred in the province of Groningen, with the highest magnitude (3.6 on the Richter scale) experienced near Huizinge in 2012. The built environment in the region consists mainly of unreinforced masonry (URM) buildings that were not designed for seismic loads and have specific characteristics, such as very slender cavity walls and limited cooperation between orthogonal walls, which limit their seismic performance. In this context, the Nederlandse Aardolie Maatschappij (NAM), an exploration and production company composed of a joint venture of Shell, Exxon and Dutch government, initiated in 2014 a comprehensive research program with experimental testing and computational modelling to assess the seismic behaviour of these URM masonry buildings (Graziotti et al 2016, Messali et al 2018, Rots et al 2017).

Among common assessment methodologies, nonlinear static (pushover) analyses represent a good compromise between linear methods and full dynamic nonlinear analyses and are able to provide

---

<sup>1</sup>Postdoctoral Researcher, Delft University of Technology, Department 3MD, [F.Messali@tudelft.nl](mailto:F.Messali@tudelft.nl)

<sup>2</sup>PhD Candidate, Delft University of Technology, Department 3MD, [M.Pari@tudelft.nl](mailto:M.Pari@tudelft.nl)

<sup>3</sup>Postdoctoral Researcher, Delft University of Technology, Department 3MD, [R.Esposito@tudelft.nl](mailto:R.Esposito@tudelft.nl)

<sup>4</sup>Full Professor, Delft University of Technology, Department 3MD, [J.G.Rots@tudelft.nl](mailto:J.G.Rots@tudelft.nl)

<sup>5</sup>Engineering Manager Structural Upgrading NAM Groningen project, NAM BV, [dick.denhertog@shell.com](mailto:dick.denhertog@shell.com)

reliable estimates of the seismic performance of URM structures. As a consequence they are usually included in the international standards and guidelines for the assessment of existing buildings (FEMA 2000, CEN 2005a, MIT 2008, ASCE 2014, NZSEE 2017). Also in the Netherlands, the draft version of the Dutch guidelines for the seismic assessment of existing buildings includes a specific section on the use of pushover analysis (NEN 2017a).

Within this context, in early 2017 a quasi-static cyclic pushover test on a calcium silicate element assemblage was carried out at Delft University of Technology as part of the large-scale testing campaign performed during 2016-17 under the NAM Structural Upgrading project (Esposito et al 2018). The assembled structure (a two-storey house composed of calcium silicate element masonry walls and concrete floors) is representative of a typical terraced house built after the 1980's in the Netherlands. The geometry of the assemblage was designed to investigate the influence of several building characteristics, such as the presence of slender piers and long transversal walls, the limited connection between the concrete floor and the walls and between the piers and the transversal walls. Walls and piers were constructed from large calcium-silicate elements with thin-layer joints. The test was selected for a blind prediction contest and nine engineering consultants working for the seismic assessment of the Groningen building stock participated in the contest. The contest aimed primarily at (i) sharing the knowledge between consultant companies, (ii) improving the understanding of the structural behaviour of a typical URM structure, and (iii) contributing to the development of the Dutch guidelines for the seismic assessment of existing buildings.

Blind prediction contests have already been used in the past to evaluate the influence of aleatory and epistemic uncertainties on the outcomes of structural nonlinear analyses. The benchmark can consist of single structural components (De Boer 2018), but more often of complex large assemblages, especially reinforced concrete structures (Combesure et al 2001, Sattar et al 2013, Richard et al 2015). As regards masonry, the behaviour of both framed masonry (Kagermanov and Ceresa 2017) and URM structures (Mendes et al 2017, De Felice et al 2017) have been analysed. For the latter, the performed contest showed that large differences may be expected between different predictions and also between the predictions and the experimental outcomes for both stone and brick URM structures. The current paper includes an overview of the experimental results, with specific focus on the test capacity curve and the evolution of the failure mechanism. The results provided by the nine engineering consultants are then presented (in anonymous format) and compared with each other and with the experimental results. The discussion is mainly focused on the adopted methodology in terms of modelling assumptions, choice of the material parameters and consequent outcomes. Finally, the applicability of the pushover assessment for the considered structure, according to the different methods recommended by the international standards and the Dutch guidelines, is discussed.

## **2. PUSHOVER TESTS ON A TWO-STOREY MASONRY ASSEMBLAGE**

A detailed description of the experiment and its outcomes is provided in Esposito et al (2018).

### ***2.1 Description of the experiment***

The geometry of the assemblage was designed to be representative of the structure, a typical terraced house built in the north of the Netherlands, characterized by the presence of slender piers, two on each façade, in combination with long transversal walls (Figure 1). The specimen was composed of single wythe walls constructed of large calcium silicate (CS) element masonry. CS12 elements and thin mortar layers with high compressive resistance were used. The standard size of the elements was 897x643x100 mm<sup>3</sup> for the piers, and 897x643x120 mm<sup>3</sup> for the transversal walls. Corresponding to the construction practice in the Netherlands, the width of some elements was customized in the factory to enable a stretcher bond between the elements at every row. Likewise, for some rows, the height of the elements was adjusted in factory to fit the desired story height. A kicker course layer was placed as 'foundation' under each wall, to smoothen possible small level differences in the underlying construction until a horizontal level was achieved. For the kicker course, smaller sized CS units, also

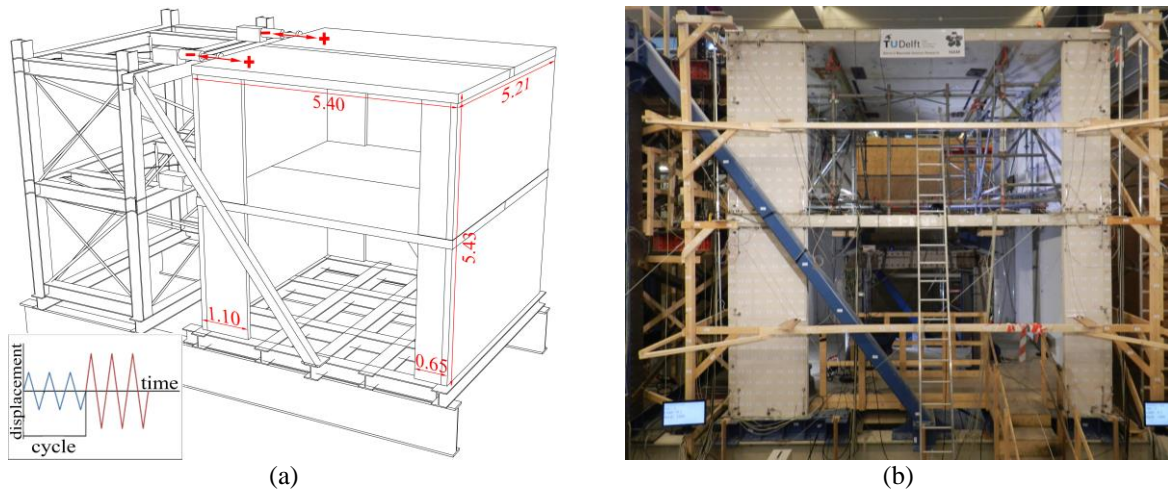


Figure 1. Two-storey masonry assemblage: (a) schematic 3D view (measures in m), and (b) the real structure before testing (b)

in CS12 quality, were used and glued to the steel foundation with high performance glue to avoid sliding at this location. This layer was clamped in both directions and failure was expected to start only from the bed joints on top of the course. At the first floor, these elements were placed on a layer of general purpose mortar. For practical reasons, each prefab massive concrete floor consisted of two parts that acted together as a single slab thanks to an in-situ casted concrete joint with carbon fibre external reinforcement strips. Both top and first floor slabs were supported by the load-bearing transverse walls and by the piers; however only the transversal wall carried the load of the floor. With large elements it is not common to have running bond at wall-pier corners; for this reason, anchor strips were used at every bed-joint level (except those between the pier elements and either the kicker course or the concrete floors). The quasi-static cyclic test was performed using a contrast frame supplied with four horizontal actuators, two at each floor level, positioned on the transversal wall side at approximately one metre inwards from the facades with piers. The house was cyclically loaded by all four actuators: the sum of the forces at the top level was maintained equal to the sum of the forces at the first level, and the displacement at the top floor was applied with cycles of increasing amplitude. The displacements of the top floor at the positions of the actuators were maintained equals to limit possible torsional rotations of the structure.

## 2.2 Overview of test results

The capacity curve of the assembled structure is shown in Figure 2 together with the corresponding backbone curve. The loading history can be divided in four phases. The elastic phase (blue line) is characterised by linear elastic behaviour of the specimen with initial stiffness of the structure equal to 21 and 25 kN/mm for negative and positive loading, respectively. The elastic phase ends when the first cracks were measured via potentiometers at the floor-to-wall connections (mainly in the facades, but also on the transversal walls). In the pre-peak phase (red curve), the cracks at the floor-wall connections became visible and the piers of both storeys started rocking, resulting in a gradual decrease in stiffness of the structure. During the peak phase (green line), the peak resistance of the building was achieved for negative displacements (-68.1 kN at a displacement of the top floor equal to -8.6 mm) when the rocking mechanism of the piers at both storeys was fully active. Meanwhile, some cracks appeared also in the transversal walls. During the post-peak phase (purple line), the peak strength was achieved also for positive loading (65.7 kN at 14.9 mm), the rocking failure mechanism localised at ground floor (soft storey mechanism) and extensive cracks appeared on the transversal walls. The post-peak phase ends when both the long piers at ground floor in the façades collapsed, causing a large reduction of the base shear force. It should be remarked that the applied loading procedure was meant to assess specifically the in-plane behaviour of the structure, and the long transversal walls only deformed in the out-of-plane direction to accommodate the in-plane deformation of the piers.

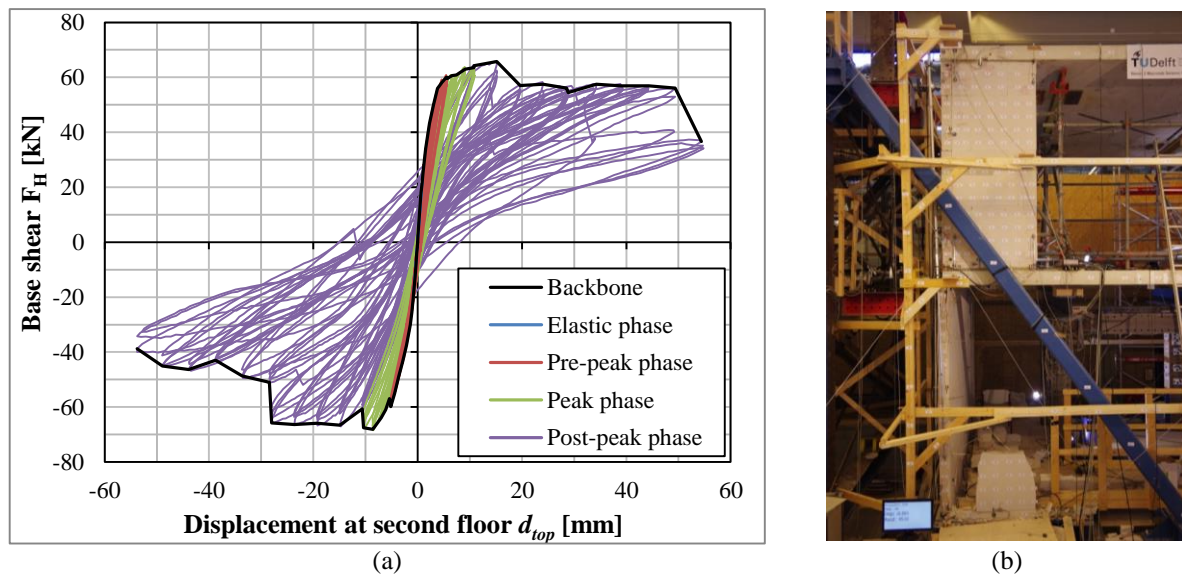


Figure 2. Base shear vs. top displacement (capacity curve) of the tested structure (a), and detail of the structure after the failure of the long piers of ground floor (b)

### 3. CONSULTANT PREDICTIONS

The consultants who participated in the blind prediction contest were provided with the geometry of the structure, the material properties (Young's modulus, tensile and compressive strength of CS elements and concrete; flexural and initial shear strength; dry friction of the joints), the construction details, and the loading procedure. The material properties were partly derived by companion tests on the masonry elements (Esposito et al 2018).

No specific requirements were given to the participants as for the choice of the modelling technique. However, they had been asked to provide the following information:

- A clear description of the used analysis method, the type of model, the software, etc., including the background reasoning behind modelling assumptions.
- The complete diagram of base shear versus second floor displacement. Specific attention was required for both push and pull direction to first cracking (end of the fully elastic stage), peak load, and near collapse, defined according to Eurocode 8 – part 3 (CEN 2005b).
- The complete diagram of base shear versus first floor displacement.
- A clear description and explanation of the failure mechanism, including the crack patterns at 75% of the peak load (pre-peak) and at near collapse.

Nine consultants participated in the contest, submitting sixteen predictions (each consultant could submit an unlimited number of predictions, but a definitive prediction for the contest had to be selected). Different modelling approaches, software packages, type of structural analysis, and assessment criteria were adopted to predict the pushover behaviour of the tested structure. The modelling approaches from the submissions can be divided in three categories:

- Continuum finite element method (fem) models: four fem models used a macro-modelling approach, with smeared crack elements, and two a simplified micro-modelling strategy, with a combination of solid and contact elements.
- Equivalent Frame (EF) models: seven models discretized the structure according to an Equivalent Frame strategy.
- Analytical-based models: three predictions were obtained on the basis of simplified techniques founded on analytical models implemented in spreadsheets.

Three consultants included more than one approach in order to compare and validate the outcomes of

their definitive prediction. Seven different software packages were used: 3Muri, Abaqus FEA, ANSR-II, DIANA FEA, ETABS, LS-DYNA and VecTor 2. Both implicit and explicit solvers were used.

The near collapse displacement was provided directly by the FEM software in case of continuum finite element models. For equivalent frame and analytical-based models the near collapse displacement was computed either on the basis of standard recommendations (ASCE 2014, CEN 2005b) or according to expertise of the analyst. Also different types of structural analysis were presented: the most of analysts submitted monotonic and cyclic static pushover analyses, but time analyses were required for explicit solvers.

### 3.2 Performance of the predictions

In the following, the performance of the provided predictions are evaluated according to the ability to identify the cracking evolution and the failure mechanism (qualitative behaviour), or to define the complete capacity curve of the structure (quantitative behaviour). Only the definitive prediction of each consultant is considered in the discussion.

As described in section 2.2, the structural behaviour of the tested building was characterized by rocking of the four piers at both storeys (peak load mechanism), followed by the mechanism localization at ground floor and the consequent failure of the long piers. All the consultants except one were able to identify properly the rocking mechanism that caused the peak strength of the structure, but only four out of nine could accurately describe the collapse of the long piers at ground floor. Other four predictions identified different failure mechanisms and one predicted no failure of the specimen until the end of the test. A summary of the predictions provided by each consultant is presented in Table 1 and examples of the identified failure mechanism are shown in Figure 3. A comparison between the experimental and the predicted capacity curves is shown in Figure 4. For consultants applying a cyclic loading protocol, the backbone curve is considered.

Overall, a large dispersion of the estimated capacities is observed. The estimated peak strength ranges between 21.3 kN and 110.2 kN (COV = 51%) for negative loads, and between 32.3 kN and 108.6 kN

Table 1. Prediction of the structural mechanisms at peak load and at failure

	<b>Prediction type</b>	<b>Peak load mechanism</b>	<b>Failure mechanism</b>
Experiment	-	Rocking of piers at both storeys	Collapse of long piers at ground story; cracking in the transversal walls
Consultant 1	Finite element model	Rocking of piers at both storeys	No failure expected before the end of the test ( $\pm 65\text{mm}$ )
Consultant 2	Finite element model	Rocking of piers at both storeys	Collapse of long piers at ground story; cracking in the transversal walls
Consultant 3	Equivalent frame model	Rocking of piers at both storeys	Diagonal cracks of long piers at both stories; cracking in the transversal walls
Consultant 4	Finite element model	Rocking of piers at both storeys	Collapse of long piers at ground story; cracking in the transversal walls
Consultant 5	Finite element model	Rocking of piers at both storeys	Diagonal cracks and collapse of every pier at ground story; cracking in the transversal walls
Consultant 6	Equivalent frame model	Rocking of piers at both storeys	Collapse of long piers at ground story; cracking in the transversal walls
Consultant 7	Finite element model	Rocking of piers at second storey	Collapse of long piers at second story
Consultant 8	Analytical based model	Rocking of piers at both storeys	Collapse of long piers at ground story; cracking in the transversal walls
Consultant 9	Equivalent frame model	Rocking of piers at both storeys	Diagonal cracks of long piers at both stories; reaching of the maximum drift for rocking piers

(COV = 42%) for positive loads. Similar results are obtained for the predictions of the displacement at near collapse (COV = 32% and 41% for negative and positive displacements, respectively) and even the predictions of the elastic behaviour of the structure were extremely scattered (COV = 78% and 35% for the negative and positive initial stiffness, respectively). This large variability may depend not only on the use of either the uncracked or the cracked Young's modulus of masonry, but also on the different assumptions related to the connections between normal walls and between floors and walls, and hence to the redistribution of the gravity loads on the piers or on the transversal walls (frame effect). The average values of the predicted initial stiffness, cracking load, peak force and near collapse displacements are close to the respective experimental values (with the exception of the positive cracking load), as reported in Table 2 and shown graphically in Figure 5 throughout a simplified segmented capacity curve. Table 2 lists also the average values and the coefficient of variation computed for groups of predictions with the same typology of analysis. Even though the dispersion of results is rather high within each group, with the obvious exception of the analytical based predictions (since only one of those was submitted as definitive prediction), some general trends can be observed. The analyses based on equivalent frame models underestimate the experimental capacity in terms of both force (peak load) and displacements (near collapse). The continuum finite element models provide a small overestimation of the peak strength and slightly underestimate the ultimate displacement capacity. On the opposite, the single analytical based model underestimates the capacity in terms of forces and overestimates in terms of displacements.

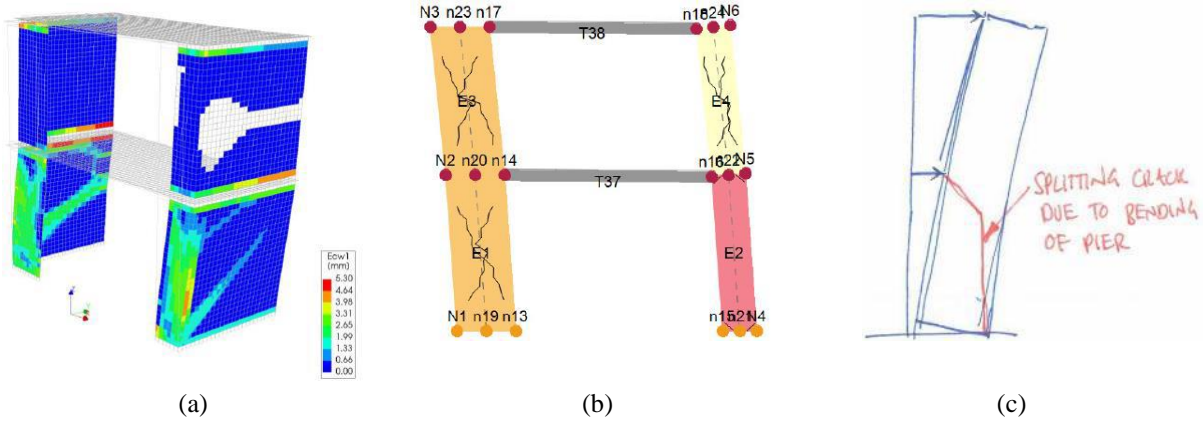


Figure 3. Examples of the predicted failure mechanism for continuum finite element (a), equivalent frame (b), and analytical based (c) models

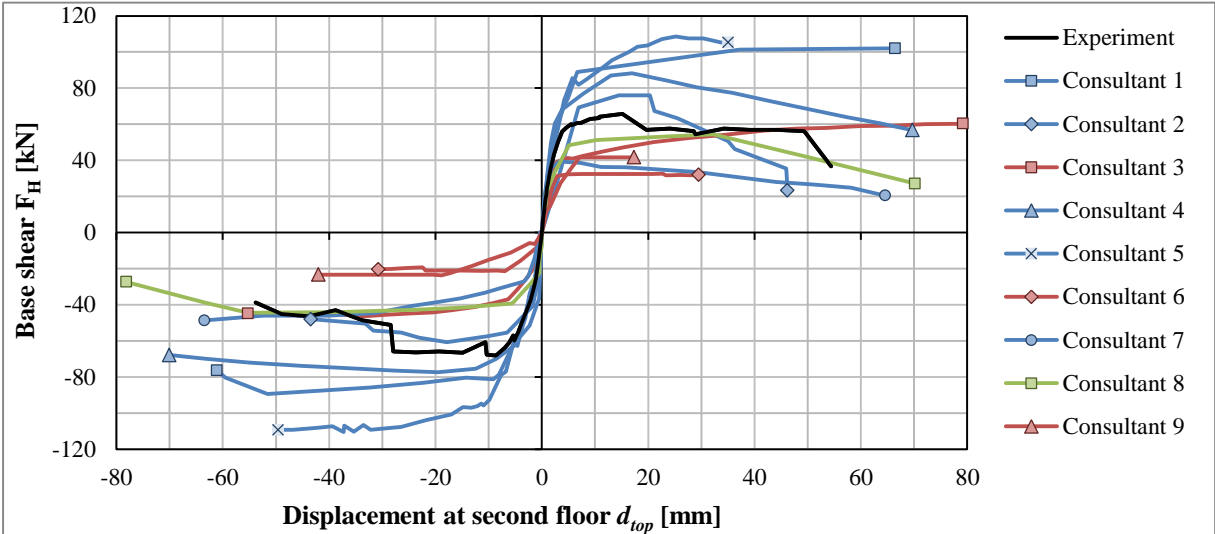


Figure 4. Experimental and predicted capacity curves of the structure (blue = finite element models; red = equivalent frame models; green = analytical based models)

Table 2. Significant displacements and forces of the capacity curve: comparison between experimental and predicted results grouped for analysis typology

Prediction type	Negative loading				Positive loading				
	$K_{in}$ [kN/mm]	$F_{cr}$ [kN]	$F_P$ [kN]	$d_u$ [mm]	$K_{in}$ [kN/mm]	$F_{cr}$ [kN]	$F_P$ [kN]	$d_u$ [mm]	
Experiment	21.1	29.5	68.1	56.3	25.0	22.1	65.7	56.9	
Every prediction	$\mu$	17.6 (-17%)	23.2 (-21%)	58.0 (-15%)	51.5 (-8%)	20.3 (-19%)	37.9 (+72%)	66.9 (+2%)	51.2 (-10%)
	COV	78%	66%	51%	32%	35%	59%	42%	41%
Analytical based model	$\mu$	48.6 (+130%)	22.4 (-24%)	44.9 (-34%)	78.1 (+47%)	24.7 (+17%)	22.4 (+1%)	54.2 (-17%)	70.2 (+23%)
	COV	-	-	-	-	-	-	-	-
Equivalent frame model	$\mu$	10.9 (-49%)	10.6 (-64%)	30.3 (-56%)	42.3 (-25%)	18.6 (-12%)	19.4 (-12%)	44.7 (-32%)	42.7 (-25%)
	COV	107%	61%	46%	28%	30%	84%	32%	75%
Finite element model	$\mu$	15.4 (-27%)	30.9 (+5%)	77.3 (+13%)	51.8 (-8%)	21.3 (+1%)	47.1 (+113%)	82.7 (+26%)	52.8 (-7%)
	COV	34%	52%	29%	29%	37%	37%	33%	21%

$K_{in}$  = initial stiffness;  $F_{cr}$  = cracking load;  $F_P$  = peak load;  $d_u$  = displacement at near collapse

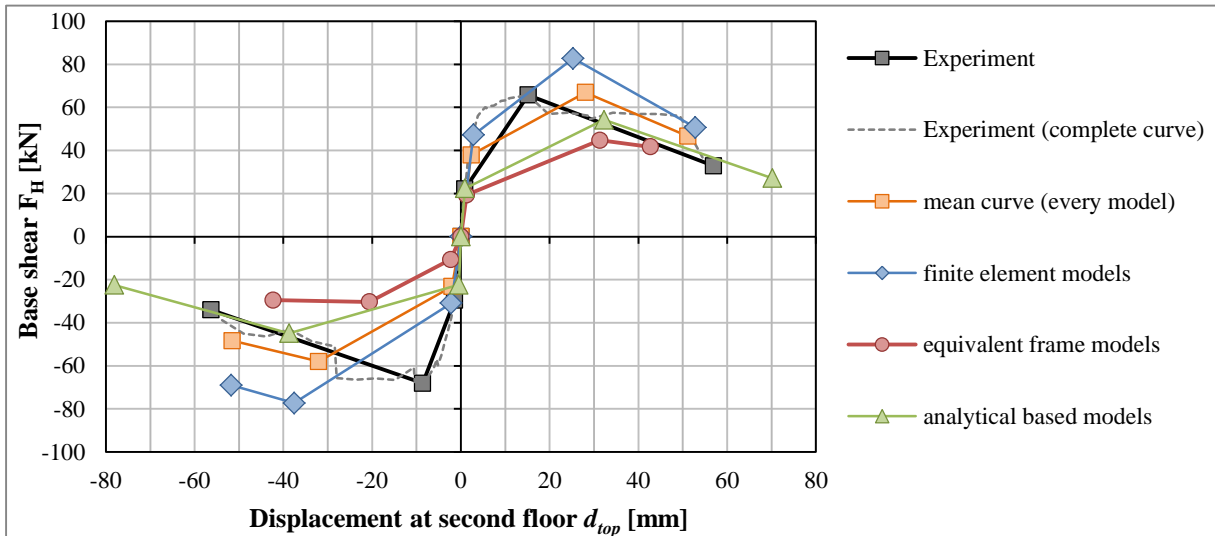


Figure 5. Simplified capacity curve of the structure: comparison between experimental and predicted results grouped for analysis typology

Also the assumptions made by each analyst on the basis of his/her expertise must be considered among the epistemic uncertainties and discussed. With finite element analyses, the material constitutive model and the related parameters (such as the tensile resistance of the masonry) can strongly influence the estimation of the peak load of the structure. Similarly, the type of solver (implicit or explicit) may affect the stability of the solution and lead to different guesses of the displacement of the structure at near collapse. When an equivalent frame approach is used, the possible redistribution of the axial load in the piers (frame effect) and the role of the transversal walls (flange effect) should be carefully evaluated, since they may not be taken into account automatically by the software. Finally, the analytical based methods require the choice of a suitable static scheme and this choice may be critical even for structures with simple geometry, such as the investigated building. When more complex structures are studied, more assumptions based on the analyst judgement are necessary (e.g. effectiveness of the connections), and more uncertainties are introduced. The combination of different modelling approaches (even a simple hand calculation based on analytical models) may hence provide



the most accurate predictions and prevent from overlooking oversights and clear mistakes. This is confirmed by the accuracy of the mean capacity curve of the structure (Figure 5), which is the closest to the experimental curve. Besides, the three consultants (#2, #4, and #8) that combined more than one approach were among those able to provide accurate predictions as regards both capacity curve and crack pattern evolution.

### 3.3 Pushover assessment

The blind prediction contest was focused on the in-plane quasi-static behaviour of the structure to evaluate the reliability of non-linear pushover (NLPO) analyses for the assessment of a typical terraced house. Hence, the capacity curves obtained from the experimental test and the numerical predictions were assessed according to the NLPO procedure presented in the Dutch guidelines NPR 9998 (NEN 2017a) for a representative location in the town of Loppersum, situated next to Huizinge and Westeremden, where the strongest earthquakes in the area were recorded in 2012 and 2006, respectively. The assessment procedure was performed according to the recommendations reported in NPR 9998 (NEN 2017a). The elastic seismic response spectrum was derived on the basis of the Uniform Hazard Spectrum (UHS) provided by the Webtool NPR 9998 (NEN 2017b) for the GPS coordinates (53.33; 6.75), and the related elastic acceleration-displacement response spectrum (ADRS) curve was derived. The procedure recommended in NPR 9998 (NEN 2017a) is based on the ‘equivalent linearization approach’ for the capacity spectrum method (CSM), initially proposed for reinforced concrete structures in ATC-40(1996), and on the ‘substitute structure’ concept assessment, defined for masonry by Magenes and Calvi (1997) for single degree of freedom (SDOF) systems. In this paper, also the general N2 method proposed by Fajfar (1999), adopted by the Eurocode 8 – part 3, and a recent alternative formulation, named  $\beta$ -corrected N2 method (Graziotti et al 2014), are considered, and the outcomes of the three assessment procedures are compared.

The capacity curve of each equivalent SDOF system was computed assuming the effective mass equal to the total mass of the structure (32.9 t) and a unit participation factor  $\Gamma$ , since a uniform loading distribution is applied and a soft storey mechanism that involved the whole structure was observed. No torsional amplification of the demand was considered, because any torsion of the building was strongly limited by the loading protocol described in section 2.1. The displacement capacity at near collapse was computed as the lateral displacement of the top floor at which one of the following conditions are met, as recommended in NPR 9998 (NEN 2017a):

- the mechanisms identified by the analyses result in the collapse of the structure;
- the base shear force sustains more than 50% degradation;
- the drift of the structure, computed at effective height or as inter-storey drift, exceeds lumped global limits (1.5% and 0.8% for inter-storey drift and drift at effective height, respectively, when the failure mechanism is ductile, such as for pier rocking).

As regards the CSM, the overdamped ADRS curve was derived by multiplying the elastic ADRS spectrum with a spectral reduction factor  $\eta_{\xi}$ , as recommended in NPR 9998 (NEN 2017). The equivalent viscous damping ( $\xi_{sys}$ ) is estimated equal to 30%, including a lumped contribution attributable to the soil-structure interaction ( $\xi_{soil} = 10\%$ ). As for the N2 method, the ultimate displacement capacity was taken as the top floor displacement at which the total lateral resistance (base shear) dropped below 80% of the peak resistance, as suggested in EN 1998 – part 3 (CEN 2005b), or by the maximum displacement of the capacity curve when such strength degradation was not observed. The initial stiffness and the related period  $T^*$  of the idealized equivalent SDOF system were computed for a shear strength equal to 70% of the peak load, as recommended in the Italian standards (MIT 2008). The corner period  $T_c$  (0.618 s) was obtained from the elastic response spectrum corresponding to the used UHS data. The determination of the target displacement is then performed according to the procedure described in Informative Annex B of EN 1998 – part 1 (CEN 2005a). The structure is then verified when the capacity over demand is larger than one and when the maximum displacement of the capacity curve is larger than 150% of the target displacement regardless of the related shear force (as required in section 4.3.3.4.2.3). Additionally, the value of the strength reduction factor R may be limited, since the elastic and inelastic target displacements may differ significantly

when the value of R is large (FEMA 2000). The Italian standards sets a maximum limit  $R = 3$  for URM buildings at Significant Damage (MIT 2008), that may be expressed as  $R=4$  at near collapse, but no direct limitations are provided in other standards as far as the author is aware. Finally, the  $\beta$ -corrected N2 method adopts the same procedures described for the standard N2 method but proposes a different equation to compute the inelastic target displacement based on the use of an exponential conversion factor  $\beta$  that amplifies the demand in case of high values of R (Graziotti 2014). The values  $\beta = 1.0$  and  $\beta = 1.8$  are used for  $R \leq 2$  and  $R > 2$ , respectively.

The capacity over demand (C/D) ratios obtained by the seismic assessment of the structure according to the three abovementioned procedures is presented in Table 3 for the experiment and each numerical prediction. Table 4 includes the average C/D values for the different groups of analysis typology. The C/D values computed on the basis of the experimental capacity curve are larger than one for both loading directions and for every assessment procedure; hence, in the considered location, the structure would be verified for in-plane loading according to NPR 9998 (NEN 2017a). Also most of the numerical predictions result in the same outcome, but large scatter of the results and some inconsistencies are observed. It is also remarkable that the definition of the capacity is frequently governed by the global drift limits at near collapse (Figure 6).

As for the analysis typology, the overall underestimation of both strength and displacement capacities given by equivalent frame models (mentioned in section 3.2) result in C/D ratios smaller than one for two of the three evaluated models (3/3 if the  $\beta$ -corrected N2 procedure is applied). On the contrary, the overestimation of the base shear identified by many continuum finite element models does not lead to large overestimation of the C/D ratio.

Table 3. Seismic assessment of the tested structure according to three different assessment procedures: comparison between the experimental outcomes and the numerical predictions

Prediction type	Negative loading			Positive loading		
	CSM	N2 method	$\beta$ -corrected N2 method	CSM	N2 method	$\beta$ -corrected N2 method
	C/D	C/D	C/D	C/D	C/D	C/D
Experiment	1.16	2.77	1.88	1.18	3.11	2.19
Consultant 1 Finite element model	1.18 (+2%)	1.99 (-28%)	1.99 (+6%)	1.23 (+4%)	2.65 (-15%)	2.65 (+21%)
Consultant 2 Finite element model	1.13 (-3%)	1.68 (-39%)	1.18 (-37%)	1.15 (-3%)	2.39 (-23%)	1.51 (-31%)
Consultant 3 Equivalent frame model	1.16 (0%)	1.26 (-55%)	0.60 (-68%)	1.19 (+1%)	1.16 (-63%)	0.69 (-68%)
Consultant 4 Finite element model	1.27 (+9%)	2.14 (-23%)	2.76 (+47%)	1.26 (+7%)	1.64 (-47%)	2.58 (-18%)
Consultant 5 Finite element model	1.52 (+31%)	2.08 (-25%)	2.08 (+11%)	1.44 (+22%)	2.26 (-27%)	2.26 (-3%)
Consultant 6 Equivalent frame model	0.78 (-33%)	0.72 <sup>1</sup> (-74%)	0.26 (-86%)	0.80 (-32%)	1.23 <sup>1,2</sup> (-60%)	0.72 (-67%)
Consultant 7 Finite element model	1.16 (0%)	0.79 (-71%)	0.79 (-58%)	1.08 (-8%)	2.77 <sup>1</sup> (-11%)	2.77 <sup>1</sup> (-26%)
Consultant 8 Analytical based model	1.15 (-1%)	1.64 <sup>1</sup> (-41%)	0.85 <sup>1</sup> (-55%)	1.16 (-2%)	1.82 (-41%)	1.02 (-53%)
Consultant 9 Equivalent frame model	0.54 (-53%)	0.55 <sup>1</sup> (-80%)	0.55 (-71%)	0.55 (-53%)	1.03 <sup>1</sup> (-67%)	0.24 (-89%)

<sup>1</sup> The strength reduction factor R is larger than 4.

<sup>2</sup> The capacity curve drops to zero strength before the 150% of the target displacement.

C/D = capacity over demand ratio; CSM = capacity spectrum method

As regards the assessment procedures, both the N2 methods are marked by larger dispersion of the results, especially the  $\beta$ -modified method. For these two procedures, since the definition of the target displacement is related to the predicted initial stiffness of the structure, the predictions not only of the capacity, but also of the demand are scattered. The introduction of the exponential conversion factor in the  $\beta$ -corrected N2 method (that results in the amplification of the inelastic demand) produces smaller values of C/D ratios, on average closer to the C/D ratio computed for the experiment; as a result, in two cases the structure would be verified when the standard N2 procedure is used but not according to the  $\beta$ -corrected method. The CSM is characterised by smaller but also less dispersed C/D ratios. In fact, the values computed for the predictions are close to the C/D ratio calculated for the experiment (-5% and -7% for negative and positive loading, respectively) with an adequately small coefficient of variation (26% and 24%). The scatter is even smaller when only the results obtained by the use of continuum finite element models are considered (COV = 13% and 11% for negative and positive loading, respectively). The small dispersion of the C/D ratios depends mainly on the stricter limitations included in the CSM method (such as the lumped spectral reduction factor), but it does not entail a better accuracy of the predictions.

Table 4. Seismic assessment of the tested structure according to three different assessment procedures: comparison between experimental and predicted results grouped for analysis typology

Prediction type	Negative loading			Positive loading			
	CSM	N2 method	$\beta$ -corrected N2 method	CSM	N2 method	$\beta$ -corrected N2 method	
	C/D	C/D	C/D	C/D	C/D	C/D	
Experiment	1.16	2.77	1.88	1.18	3.11	2.19	
Every prediction	$\mu$	1.10 (-5%)	1.43 (-48%)	1.23 (-35%)	1.10 (-7%)	1.88 (-39%)	1.60 (-27%)
	COV	26%	43%	69%	24%	35%	61%
Analytical based model	$\mu$	1.15 (-1%)	1.64 (-41%)	0.851 (-55%)	1.16 (-2%)	1.82 (-41%)	1.02 (-53%)
	COV	-	-	-	-	-	-
Equivalent frame model	$\mu$	0.83 (-29%)	0.97 (-65%)	0.53 (-72%)	0.85 (-28%)	1.48 (-52%)	0.78 (-64%)
	COV	38%	38%	35%	38%	7%	34%
Finite element model	$\mu$	1.25 (+8%)	1.74 (-37%)	1.76 (-6%)	1.23 (+4%)	2.34 (-25%)	2.35 (+7%)
	COV	13%	32%	44%	11%	19%	22%

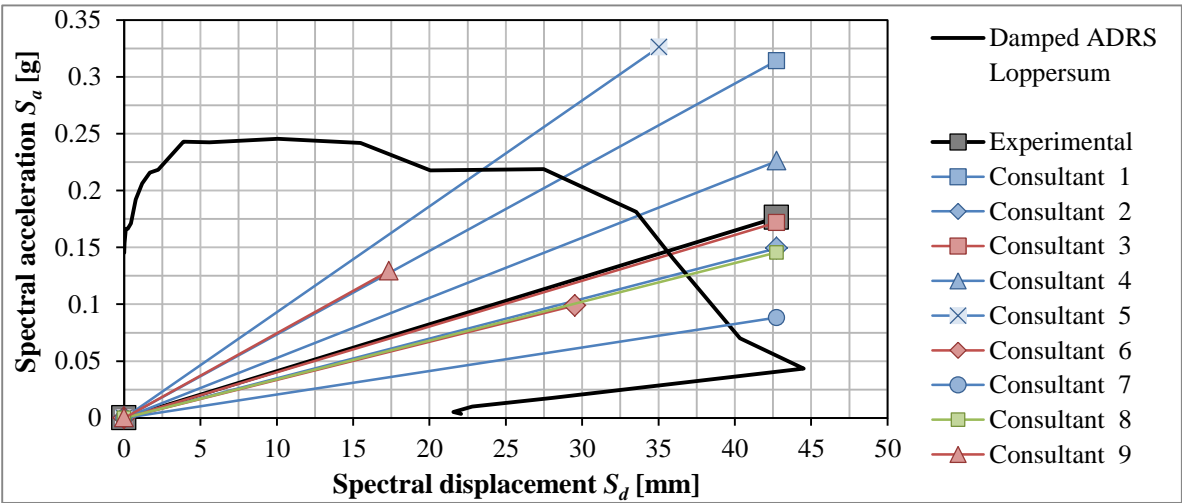


Figure 6. Graphical seismic assessment based on CSM: comparison between the experimental and the numerical predictions for positive loading (blue = fe model; red = EF model; green = analytical based model)

## 4. CONCLUSIONS

In recent years, induced seismicity in the Netherlands has considerably increased. The Nederlandse Aardolie Maatschappij (NAM) started in 2014 a comprehensive research program with experimental testing and computational modelling to assess the seismic behaviours of URM masonry buildings. In this framework, a quasi-static cyclic pushover test on a calcium silicate element assemblage was carried out in early 2017 at Delft University of Technology. The test was selected for a blind prediction contest with the aim of (i) sharing the knowledge between consultant companies, (ii) improving the understanding of the structural behaviour of a typical URM structure, and (iii) contributing to the development of the Dutch guidelines for the seismic assessment of existing buildings. Nine engineering consultants working for the seismic assessment of the Groningen building stock participated to the contest. The consultants adopted several methods to predict the behaviour of the tested structure: three modelling approaches (finite element models, equivalent frame models, analytical-based models); seven software packages; different assessment criteria, loading protocols, and types of structural analysis.

From a qualitative point of view, almost every consultant was able to identify the primary failure mechanism that determined the peak strength of the structure, but only four out of nine described properly the final collapse mechanism (specifically, consultants 2, 4, 6, and 8). As regards the prediction of the capacity curve of the building, large dispersion was observed but the mean predicted initial stiffness, cracking load, peak force and near collapse capacity were close to the respective experimental values. The large variability depends on both the use of different modelling approaches and on the specific assumptions made for modelling the details of the structure (e.g. wall-pier connections). The combination of more than one approach allows to compare and cross-validate the results and hence to provide more accurate predictions. For this purpose, even simple hand calculation based on analytical models prevent from overlooking oversights and clear mistakes.

The received predictions have been used to assess the seismic vulnerability of the tested structure according to the recent Dutch seismic guidelines and with different assessment procedures. The data analysis shows that, despite the different predictions of the capacity curves, the assessments based on the numerical analyses were overall consistent to that based on the experimental outcomes, especially with finite element models and when the CSM is used.

The blind prediction contest was hence useful to evaluate the modelling and the assessment procedures, and to provide the consultants working for the seismic assessment of the Groningen building stock with some useful information on how to refine their analyses. Finally, it contributed to a critical evaluation of the assessing procedure recommended in the Annex G of the Dutch guidelines NPR 9998.

## 5. ACKNOWLEDGEMENTS

This research was funded by NAM, under the contract number UI63654 “Testing program 2016 for Structural Upgrading of URM Structures”, which is gratefully acknowledged.

## 6. REFERENCES

- ASCE American Society of Civil Engineers (2014), *Seismic Evaluation and Retrofit of Existing Buildings* (ASCE/SEI 41 13). Reston, VA, United States
- ATC, Applied Technology Council (1996). *ATC-40 Seismic evaluation and retrofit of concrete buildings*. Applied Technology Council report. Redwood City.
- CEN, European Committee for Standardization (2005a), *Design of structures for earthquake resistance-part 1: general rules, seismic actions and rules for buildings*, Design Code EN 1998-1. Brussels, Belgium

- CEN, European Committee for Standardization (2005b), Design of structures for earthquake resistance-part 3: Assessment and retrofitting of buildings, Design Code EN 1998-3. Brussels, Belgium
- Combescur D, Sollogoub B, Ile N, Reynouard JM, Mazars J, Naze PA (2001). CAMUS III International benchmark. Synthesis of the participant reports.
- De Boer A, Hendriks MAN, Van der Veen C (2018), Organizing an international blind prediction contest for improving a guideline for the nonlinear finite elements analysis of concrete structures, *Proceedings of EURO-C 2018*, 26 February – 01 March, Bad Hofgastein, Austria
- De Felice G, De Santis S, Lourenço PB, Mendes N (2017). Methods and Challenges for the Seismic Assessment of Historic Masonry Structures. *International Journal of Architectural Heritage*, 11(1), 143-160.
- Esposito R, Safari S, Ravenshorst GJP, and Rots JG (2018). Characterisation of calcium silicate brick and element masonry structures. *Proceedings of 10th Australasian Masonry Conference*, 11-14 February, Sidney, Australia
- Fajfar P (1999). Capacity spectrum method based on inelastic demand spectra. *Earthquake Engineering & Structural Dynamics*, 28, 979-993.
- FEMA, Federal Emergency Management Agency (2000). Prestandard and commentary for the seismic rehabilitation of buildings. Report FEMA-356, Washington, DC.
- Graziotti F, Penna A, Bossi E, Magenes G (2014). Evaluation of displacement demand for unreinforced masonry buildings by equivalent SDOF systems. Proceedings of the 9th International Conference on Structural Dynamics (EURODYN 2014), 30 June – 2 July 2014, Porto, Portugal.
- Graziotti F, Rossi A, Mandirola M, Penna A, Magenes G. (2016). Experimental characterization of calcium-silicate brick masonry for seismic assessment. *Proceedings of 16th International brick/block masonry conference*, 26-30 June 2016, Padova, Italy.
- Kagermanov A, Ceresa P (2017). Blind Prediction of a Three-Storey RC Frame Building with Masonry Infill Walls. Proceedings of 7th International Conference on Advances in Experimental Structural Engineering (AESE), 6-8 September, Pavia, Italy.
- Magenes G, Calvi GM (1997). In-plane seismic response of brick masonry walls. *Earthquake engineering & structural dynamics*, 26(11), 1091-1112.
- Mendes N, Costa AA, Lourenço PB, Bento R, Beyer K, de Felice G, et al (2017). Methods and approaches for blind test predictions of out-of-plane behavior of masonry walls: A numerical comparative study. *International Journal of Architectural Heritage*, 11(1), 59-71.
- Messali F, Esposito R, Jafari S, Ravenshorst G, Korswagen P, Rots J (2018). A multiscale experimental characterization of Dutch unreinforced masonry buildings. *Proceedings of the 16th European Conference on Earthquake Engineering*, 18-21 June, Thessaloniki, Greece
- MIT, Ministry of Infrastructures and Transportations (2008), NTC 2008. Decreto Ministeriale 14/1/2008: Norme tecniche per le costruzioni., G.U.S.O. n.30 on 4/2/2008 (in Italian)
- NEN (2017a), NPR 9998 2017, Beoordeling van de constructieve veiligheid van een gebouw bij nieuwbouw, verbouw en afkeuren - Grondslagen voor aardbevingsbelastingen: geïnduceerde aardbevingen, draft June 2017 (in Dutch)
- NEN (2017b), <http://seismischekrachten.nen.nl/webtool.php>
- NZSEE, New Zealand Society for Earthquake Engineering (2017), The seismic assessment of existing buildings, Part C8: Seismic assessment of unreinforced masonry buildings. Wellington, New Zealand: MBIE, EQC, SESOC, NZSEE and NZGS
- Richard B, Martinelli P, Voldoire F, Corus M, Chaudat T, Abouri S, Bonfils N (2015). SMART 2008: Shaking table tests on an asymmetrical reinforced concrete structure and seismic margins assessment. *Engineering Structures*, 105, 48-61.
- Rots JG, Messali F, Esposito R, Mariani V, Jafari S (2017). Multi-Scale Approach towards Groningen Masonry and Induced Seismicity. *Key Engineering Materials*, 747: 653-661
- Sattar S, Liel AB, Martinelli P (2013). Quantification of Modeling Uncertainties Based on the Blind Prediction Contest Submissions. Proceedings of Structures Congress 2013: Bridging Your Passion with Your Profession 2-4 May, Pittsburgh, Pennsylvania, USA